Dissociable Auditory Mismatch Response and Connectivity Patterns in Adolescents with Schizophrenia and Adolescents with Bipolar Disorder with Psychosis: a Magnetoencephalography Study.

Sven Braeutigam* (1), Danai Dima (2,3,4), Sophia Frangou (4) and Anthony James (5,6)

(1) 0xford Human Brain Activity Center, Department of Psychiatry, University of Oxford, OX3 7JX, UK, sven.braeutigam@psych.ox.ac.uk, Tel: +44 (0) 1865 283816, Fax: +44 (0) 1865 793101

(2) Department of Psychology, School of Arts and Social Sciences, City, University of London, London, UK

(3) Department of Neuroimaging, Institute of Psychiatry, Psychology and Neuroscience, King's College London, UK

(4) Department of Psychiatry, Icahn School of Medicine at Mount Sinai, USA

(5) Department of Psychiatry, University of Oxford, UK

(6) Highfield Unit, Warneford Hospital, Oxford, UK

*Corresponding author

26 pages words: 5596 (total), 198 (abstract), 3019 (main text)

Abstract

Background: There is overlap between schizophrenia and bipolar disorder regarding genetic risk as well as neuropsychological and structural brain deficits. Finding common and distinct event-response potential (ERP) responses and connectivity patterns may offer potential biomarkers to distinguish the disorders.

Objective: To examine the neuronal auditory response elicited by a roving mismatch negativity (MMN) paradigm using magnetoencephalography (MEG).

Participants: 15 Adolescents with schizophrenia (ASZ), 16 adolescents with bipolar disorder with psychosis (ABP), and 14 typically developing individuals (TD).

Methods: The data were analysed using time-series techniques and dynamic causal modelling (DCM).

Outcome measures: MEG difference wave (deviant – standard) at primary auditory (~90ms), MMN (~180ms) and long latency (~300ms).

Results: The amplitude of difference wave showed specific patterns at all latencies. Most notably, it was significantly reduced ABP compared to both controls and ASZ at early latencies. In contrast, the amplitude was significantly reduced in ASZ compared to both controls and ABP. The DCM analysis showed differential connectivity patterns in all three groups. Most notably, inter-hemispheric connections were strongly dominated by the right side in ASZ only.

Conclusions: Dissociable patterns of the primary auditory response and MMN response indicate possible developmentally sensitive, but separate biomarkers for schizophrenia and bipolar disorder.

Introduction:

A shared aetiology between schizophrenia and bipolar disorder with psychosis is supported by findings from genetic (Lee et al.), neuropsychological (Hill et al., 2013), phenomenological (Tamminga et al., 2013), structural (Ivleva et al., 2012) and functional neuroimaging studies (Li et al., 2017). It is important to see if any shared aetiology is reflected in similar, or related patterns of pathophysiology in adolescent–onset cases, where neurodevelopmental processes are likely to operate.

Electrophysiological techniques (Thibaut et al., 2015) can help determine biomarkers at the neuronal level. Of particular relevance are passive event related potentials (ERPs) in response to auditory oddball paradigms. The N100, a late, attention-sensitive auditory evoked potential (AEP) (McCarley et al., 1991) and the mismatched negativity (MMN) a neurophysiological index of the disturbed automatic and pre-attentive detection of deviant information, evoked by either a change in duration, frequency, loudness, or spatial locus of origin (Näätänen et al., 1978). MMN is a highly reproducible neurophysiological marker in schizophrenia and has been shown to follow a progressive course, with reduced MMN amplitude associated with a loss of grey matter in the left superior temporal gyrus (STG) (Salisbury et al., 2007).

However, ERP measures alone appear less than clear-cut in differentiating the disorders (Näätänen et al., 2012). Reduced amplitude of early auditory ERP components (N100, P200, and N200) are seen in schizophrenia (O'Donnell et al., 2004), some report similar reductions in bipolar disorder (Wang et al., 2014), but others do not (Johannesen et al., 2013). Likewise, some studies have found common neurobiological disturbances in deviance detection/orienting processes (Kaur et al., 2011), others have reported deficits in pre-attentive auditory processing,

and MMN deficits that are less severe in bipolar disorder (Jahshan et al., 2012a). Hermens et al (Hermens et al., 2017) recently concluded that MMN was not a diagnosis specific biomarker.

Adolescence through to early adulthood is a period of intense brain re-organisation. The cortical network generating MMN continues to develop in adolescence into to adulthood (Cooray et al., 2016). Cortical regions in the temporal and frontal lobes, involved in auditory processing, mature with increasing fronto-temporal connectivity together with increased sensitivity in the temporal regions for changes in sound stimuli (Cooray et al., 2016). It is thought that at a neuronal population level this reflects a maturation of the excitatory inhibitory balance in the temporal regions. Mapping changes in adolescence may, therefore, represent a uniquely sensitive way to understand the MMN response in schizophrenia and bipolar disorder against the developmental course of adolescence (e.g., Arango et al., 2014)

Following our previous work (Dima et al., 2012) we used Magnetoencephalography (MEG) to quantify the MMN neuronal response in adolescents with schizophrenia (ASZ), in adolescents with bipolar disorder with psychosis (ABP) and in normally developing adolescents. MEG is able to image the brain at high temporal resolution, where the spatial resolution is typically better than EEG, thereby offering the potential to better delineate neural correlates of these disorders. We aimed to examine whether there are differences in early latency deviance detection/orienting processes and the MMN in the early phase between the two disorders reflecting differing neurobiological processes. In order to fully exploit the MEG data and in line with a wealth of studies suggesting schizophrenia specific effects at post-MMN latencies (e.g., Salisbury et al., 1999), we analysed an extended latency range compared to typical MMN studies.

<Table 1 about here>

2. Methods

2.1 Subjects

Fifteen adolescents with first episode schizophrenia and 16 adolescents with bipolar disorder with psychosis were recruited. All patients met DSM-IV criteria (APA, 1994) for schizophrenia or bipolar disorder with psychosis, using the Kiddie Schedule for Affective Disorders and Schizophrenia (Kaufman et al., 1997). Exclusion criteria included moderate mental impairment (IQ <70), a history of pervasive developmental disorder, substance misuse disorder, significant head injury, neurological disorder or major medical disorder (demographics see Tab. 1).

2.2 Roving mismatch negativity paradigm

Sinusoidal tones (duration: 70ms; 10ms rise/fall; inter-tone interval: 500ms) were presented binaurally in trains of length 1 to 11 tones (for an illustration see S1; supplementary materials). The trains differed in sound frequency (500-800Hz in steps of 50Hz). Both train length and frequency were pseudo-randomly chosen, but only tone trains of lengths 6 to 11 entered the analysis. The subjects were asked to respond to a visually displayed cross changing grey-scale every 2-5s by pressing a button while passively attending the tones. The experiment lasted for 15 minutes. On average, 194 ± 8 tone trains entered the analysis, each providing one standard (= 6^{th} tone; STD) and one deviant (= 1^{st} tone; DEV) stimulus. The paradigm is same as previously employed (Dima et al., 2012). For further details, the reader is referred to the work by Garrido and colleagues (Garrido et al., 2009c).

2.3 Data acquisition

Measurements were performed on the Elekta-Neuromag VectorView^{TM} system at the Oxford Centre for Human Brain Activity. The system provides 204 gradiometer channels that are most sensitive to nearby (cortical) sources, where the local root-mean-square (rms) value calculated over the two channels at each detector site and the global rms value calculated over all channels are measures of the local and global brain activity, respectively. Because of the strength (rms) property of gradiometers, the notions of ERP amplitude and neuronal activity will be used interchangeably in the following wherever possible. The data were pre-processed using signal space separation (Taulu et al., 2004) and standard projection methods to remove ocular and cardiac artefacts (e.g., Gonzalez-Moreno et al., 2014). A small number of trials (< 0.5%) were excluded because of other artefacts (muscle tension, sensor jumps, etc.) not amenable to pre-processing.

2.4 Data analysis

All epochs between -100ms to 700ms peri-stimulus were classified as either standard (STD) or deviant (DEV). Prior to analysis, the epochs were band-pass filtered between 0.5 and 40 Hz and normalized to pre-stimulus variance.

The epochs were examined using two approaches. First, an analysis of evoked amplitudes using a measure P(t) yielding significance as a function of time. P(t) is a robust measure of the differences between evoked responses in signal space and is calculated as follows. Individually for each channel, a local measure *f*(t) of the significance of differences between evoked responses across subjects is obtained, where *f* denotes a paired Wilcoxon test of matched samples applied separately to STD and DEV epochs (within group; denoted *w* in the following), or a Mann-Whitney U test applied to DEV-STD difference curves (across groups; *u*). Then, a global measure of significance across subjects is obtained according to

$$\mathrm{P}(t) = \text{probability}\left(\chi^2\right) \qquad \left(\chi^2\right) = -2\sum_{i=1}^{N} \ln\left[f_i(t)\right]$$

where N denotes the number of channels, and probability is the significance level of the quantity in brackets (Braeutigam et al., 2004; Braeutigam et al., 2008). Note that the χ^2- test controls for multiple comparisons over channels. We accepted significance at $p < 0.01$.

Second, Dynamic causal modelling (DCM) applied to standard and deviant tones for latencies up to 250 after stimulus onset (i.e., including the traditional MMN time window). As used here, DCM represents the transition in brain response from standard to deviant as a change in effective connectivity of a given network model specified by the number and type of neuronal sources, number and type (forward, backward, etc.) of effective connections, and rules determining which connections are allowed to change. A total of 12 models were sourced (see Fig. 3, inset) in order to model the MMN effect on neuronal networks including changes in symmetry and laterality of connections (Garrido et al., 2007; Garrido et al., 2008; Garrido et al., 2009a; Garrido et al., 2009b).

This choice of DCM extends our previous study (Dima et al., 2012) to include inter-hemispheric (lateral superior temporal lobe gryus STG) connections and a source in the left inferior frontal gyrus. These inclusions were suggested by the data (left frontal activity in PBD in particular) and recent insight into impaired inter-hemispheric connectivity in schizophrenia (Ribolsi et al., 2011). In line with the previous literature, DCM calculations were applied to the latency range 0 – 250ms. A list of DCM parameters is given in S2.

For each test, the best model had a Bayesian exceedance probability that was at least twice the value of all competing models, where the measure exceedance balances goodness-of-fit and model complexity. Core DCM was used as provided by SPM8

(www.fil.ion.ucl.ac.uk/spm/software/spm8/), augmented by an a-posteriori bootstrap test in order verify that exceedance differentiated robustly between groups and conditions (details are given in S3). The standard MNI template brain was used for DCM analysis.

3. Results

3.1 Behavioural measures

All 45 subjects completed the experiment successfully. On average, TD subjects identified the highest number of cross changes (89 ± 4%) and responded fastest (555 ± 47ms), followed by ASZ (81 ± 7%; 726 ± 76ms) and then ABP (76 ± 6%; 798 ± 89ms) individuals. The differences in scores and reaction times were not statistically significant ($p < 0.05$; one way ANOVA). The task performance was significantly less than 100% in all three groups ($p < 0.05$), however, there was no systematic pattern in the missed responses.

<Figure 1 about here>

3.2 Signal space analysis

In all subjects neuronal activity elicited by tones exhibited two prominent peaks of neural activity at about 90ms (primary auditory response) and 200ms (mismatch latency) after stimulus onset, respectively (Fig. 1). The signal topographies of ERPs were broadly consistent across all subjects with dominant sources in bilateral temporal and inferior frontal cortices. Evoked power decayed rapidly after about 300ms after stimulus onset in all groups.

Measure P(t) identified 3 time intervals where signals differed significantly (Fig. 2). First, deviant tones evoked significantly (measure *w*) stronger neuronal responses compared to standard tones between about 60 and 90ms after stimulus onset in both TD and ASZ. This was not the case in ABP subjects., where the difference (DEV - STD) curve was indistinguishable from baseline within this time window. Note that the amplitude of the difference curve was the same in TD and ASZ (measure *u*).

Second, deviant tones evoked significantly stronger neuronal responses compared to standard tones in all subject groups between about 130 and 200ms (mismatch negativity window) after stimulus onset (*w*). The amplitude of the difference wave was significantly smaller in ASZ compared to the other two groups (*u*).

Third, standard tones evoked significantly (*w*) stronger neuronal responses compared to deviant tones in ASZ and ABP subjects between about 230 and 290ms after stimulus onset. The effect was strongest in ABP, where the difference wave was significantly larger compared to ASZ (*u*). No significant differences between standard and deviant tones were found at this latency in TD subjects.

<Figure 2 about here>

3.3 DCM modelling

In each subject group the best model identified by a Bayesian estimator had an exceedance probability that was at least 5 times as high as the second best fit. In each case, the best model had 6 sources with modulated forward and backward connections. Across groups, however, the models

differed in terms of inter-hemispheric (lateral) connections.

In TD subjects, the most complex model (M10) best described the data, in which lateral STG connections were present and connectivity changed between the responses to standard and deviant tones (Fig. 3). A post-hoc analysis (T-test) of DCM parameters suggested that the lateral connection strengths were symmetrical in TD subjects, i.e., the right-to-left had the same magnitude as the left-right connections.

In ASZ subjects, a less complex model (M11) best described the data, in which lateral connections were present but were not required to change between standard and deviant tones in order to fit the data. The post-hoc analysis of DCM parameters suggested that lateral connection strengths were significantly asymmetrical in AOS individuals, with right-to-left connections about 2.5 times stronger than left-right connections. In ABP subjects, an even less complex model (M7) described the data, in which lateral connections were absent.

<Figure 3 about here>

3.4 Possibly confounding variables

No significant (within group) correlations were found between the electrophysiological findings and full-scale IQ in the entire sample, or in patients with medication (CPZ equivalents), and symptom severity (PANSS).

4. Discussion

This, to our knowledge, first comparative MEG study of psychosis in adolescence, where neurodevelopmental processes are operative, suggests that there are dissociable neuronal effects both at the level of event-related fields and connectivity patterns between the disorders. This may cast light upon the trajectory of shared and non-shared pathophysiology. Unfortunately, it is not easy to fully discuss these observations in the light of the previous literature, as there have been many contradictory EEG and MEG findings indicating both similarities (Kaur et al., 2011) and differences (Jahshan et al., 2012b) between schizophrenia and bipolar disorder, for the most part conducted in adults, and those with chronic illnesses. Our data suggest that early-latency cortical responses are altered in ABP patients, however, this does not appear to be the case here in adolescent schizophrenia, where the modulation of the N100-like response appears normal (both latency and topography in the early peak observed here matches the N100 features). This is seemingly at variance with other findings of an intact N100 in bipolar disorder (Onitsuka et al., 2013), and schizophrenia where a reduced amplitude of N100 is normally found (O'Donnell et al., 2004). Likewise, a previous EEG study of ASZ (Oades et al., 2006) did not report abnormalities in the N100 window. A recent study (Wang et al., 2014) found reduced M100 and M200 source strength bilaterally, which was thought to reflect similar early auditory information processing deficits in schizophrenia and bipolar disorder.

As reported in our previous study (Dima et al., 2012), the MMN amplitude was strongly reduced in patients with schizophrenia compared to typically developing subjects, while for bipolar disorder the MMN was intermediately reduced, in line with the findings of Hermens et al (Hermens et al., 2017). A recent meta-analysis (Erickson et al., 2015) found the effect size for MMN amplitude changes in schizophrenia were greater with disease progression, while that for bipolar disorder were smaller and similar to that seen in first episode schizophrenia. In another meta-analysis of FEP, Haigh et al (Haigh et al., 2017) found no MMN reduction to pitch-deviants and a small-to-medium reduction to duration-deviants, indicating a likely progression in the reduction of MMN

with time. However, here, during adolescence the reduction in MMN is significant and much greater in those with schizophrenia than bipolar disorder at the outset. A shared pathology may still be indicated because reduced MMN is related to *N*-methyl-D-aspartate receptor (NMDAR) dysfunction in schizophrenia and in first episode psychosis, and is associated with higher plasma levels of glutamate (Nagai et al., 2017).

In this context, it should be noted that MMN reduction might not be present in relatively high functioning individuals with schizophrenia (Salisbury et al., 2017), and in one meta-analysis (Haigh et al., 2017) effect sizes for the duration MMN decreased from d = 0.47 to 0.36 when IQ or education was accounted for. Although we did not observe significant correlations between the electrophysiological findings and full-scale IQ, it possible that the MMN reduction observed in ASZ relates to some extent to IQ, which was significantly lower in ASZ compared to TD.

The connectivity analysis might indicate changes at the system level. ABP subjects utilize a functionally different network (absent lateral connections) that is still capable of producing a normal MMN response assumed to reflect predictive coding, where the system reduces prediction error during stimulus repetition and dynamically adjusts error estimates following change. In contrast, ASZ subjects utilize a network with lateral connections, as in normal subjects, but the network is dynamically skewed, resulting in impaired prediction coding, hence reduced MMN amplitude (Baldeweg, 2007). These putative changes at the system level might explain the differential effect observed at longer latency most notably in ABP and to a lesser degree in ASZ patients.

Latency, signal topographies as well as the smallness of (non-difference wave) amplitudes are broadly consistent with a P3 response using a passive task (Bennington & Polich, 1999). The P3 is commonly believed to be an endogenous neuronal component that is dependent on the level of attention and arousal as well as the context in which a stimulus occurs (Polich, 2007). We

acknowledge that this interpretation may be wrong, however, the existence of dissociable effects at latencies usually associated with higher order mechanisms may further support the notion that in adolescence, an active period of brain re-organization, different developmental pathways are materializing in schizophrenia and bipolar disorder with psychosis (Arango et al., 2014).

There are limitations to this study. Most notably, the sample size is reasonable but still comparatively small making it difficult to precisely control for the effects of medication and symptom severity. This needs to be investigated more closely as it has been suggested that quetiapine can improve MMN impairments (Oranje et al., 2017), and that there are correlations with both positive symptoms (Rudolph et al., 2015) and negative symptoms (Coffman et al., 2017; Oades et al., 2006). Moreover, individual MR images were not available, which might have reduced the accuracy of the DCM estimates. Also, and this is a general problem of electrophysiological recordings, some artefacts (e.g., muscular) might not have been removed during pre-processing (e.g., Gonzalez-Moreno et al., 2014).

Despite these limitations, large robust differences in the neuronal response were found. Overall, this study points to the importance of studying adolescents in order to understand the developmental changes, and any predictive value of alterations of the neuronal response in this age group. Indeed, there may be a greater impairment of MMN with time (Erickson et al., 2016; Kaur et al., 2013), and young patients with the most impaired MMN amplitudes at baseline are reported to show the most severe levels of disability at follow-up (Kaur et al., 2013). Hence, detection of differential abnormalities in these ERPs in the earliest stages of the disease process will be important to our understanding of the development of psychosis. Indeed, this paper points to neurophysiological differences in evoked components as well as connectivity patterns between these disorders and healthy controls, and between schizophrenia and bipolar disorder with psychosis in the earliest stages of the illnesses - in adolescence at first-episode. It would be informative to extend this approach to examine the neuropsychological deficits and developmental

trajectories of cognitive functioning (Kaur et al., 2013) with longitudinal studies.

Acknowledgments

We would like to thank the participants of this study and their parents for support. This work was supported by the Department of Psychiatry, Oxford University.

Table 1

	ASZ N=15	**ABP N=16**	**TD N=14**	**Statistic**	**p**
Male/Female	9 / 6	10 / 6	6 / 8	χ^2 =1.7	0.49
Age	17.0 ± 1.0	16.8 ± 1.1	16.7 ± 1.9	$F_{2,44}$ = 0.16	0.89
Duration	0.9 ± 0.9	1.2 ± 1.3		χ^2 =0.19	0.65
R/L	15 / 0	14 / 2	12 / 1	χ^2 = 1.9	0.38
+PANSS	21.3 ± 3.0	19.5 ± 6.1		$t_{1,30}$ = 1.0	0.32
-PANSS	13.5 ± 5.1	7.5 ± 0.8		$t_{1,30}$ = 18.5	< 0.001
CPZ-Eq	251 ±140	172 ± 176		$t_{1,30}$ = 1.7	0.2
FSIQ	91.6 ± 13.9	99.3 ± 11.8	113.4 ± 8.5	$F_{2,38}$ = 9.7	< 0.001
BDI	4.2 ± 1.6	6.4 ± 1.4		t_{53} = 4.3	< 0.001
Y-MRS	0.4 ± 0.4	1.4 ± 0.8		t_{53} = 5.3	< 0.001
<u>Medication</u> Olanzapine Quetiapine Risperidone Fluoxetine Sodium Lithium Clozapine Aripiprazole	 5 0 8 1 2 0 2 1	 7 2 4 2 3 2 0 1			

Table 1 Demographic details of adolescents with schizophrenia (ASZ), adolescent with bipolar disorder with psychosis (ABP) and healthy controls (TD). Age in years. Disease duration in years at time of scanning. R/L: Handedness, Edinburgh Inventory. +/-PANSS: Positive and Negative Syndrome Scale, positive/negative scores (Kay et al., 1987). CPZ-Eq: Chlorpromazine equivalent (Leucht et al., 2015). FSIQ: Wechsler full scale IQ. BDI: Beck Depression Inventory. Y-MRS: Young Mania Rating Scale. Where applicable, <mean> ± <standard deviation of mean> are specified.

Figure captions

Figure 1. Global root-mean-square (rms) signals evoked by tones averaged over all stimuli. The curves were obtained by summation over all subjects in each group and all gradiometer channels. Tone onset is at t = 0. Typically, the tones evoked two prominent peaks of neural activity at about 90 and 220ms after stimulus onset, respectively. The amplitude of the second peak is reduced in both patient groups compared to TD subjects. The inset illustrates the distribution of neural activity (local rms-signal averaged over all subjects in each group) over the head. In general, the signal topographies (distribution of neuronal activity over the head at a given point in time) were broadly consistent across all subjects with sources in bilateral temporal and inferior frontal cortices. For the presentation of data, the MEG detectors have been projected into two dimensions (left ear on the left, front at the top). TD: typically developing healthy controls; ASZ adolescents with schizophrenia; ABP adolescents with bipolar disorder with psychosis.

Figure 2. Global rms-signal in the three subject groups based on difference waves (deviant - standard). Non-parametric time-series analysis identified three broad intervals in which neuronal responses to standard and deviant tones differed significantly. In general, amplitude differences within each interval followed a broadly similar pattern in all three groups, but effect sizes were significantly different (see 3.2 for details). The inset illustrates the distribution of differential activity (local rms-signal of the DEV – STD difference wave) over the head within the mismatch negativity window, 130 – 200ms (maps shown at peak latencies). The signal topographies were broadly consistent across all subjects with similar sources compared to non-difference event related fields, implying that the mismatch negativity response reflects modulation of activity within given regions as opposed to shift of activity from one brain area to another.

Figure 3. Dynamic causal model estimation. The panels show the SPM8 output for the three subject groups. In each case, one model is clearly favoured by the Bayesian estimator (for visual presentation, all exceedance probabilities were transformed to an inverted scale of negative logarithms, where higher values indicate higher likelihood). Vertical lines on top of the three winning models show confidence intervals based on a bootstrap test over subjects. The three models differed only with respect the lateral connections across the three subject groups. Upper left inset: Sources used for dynamic causal modelling (DCM) calculations superimposed on the MNI template brain (left primary auditory cortex A1 [-42, -22, 70], right A1 [46, -14, 8], left superior temporal gyrus STG [-61, -32, 8], right STG [59, -25, 8], left inferior frontal gyrus IFG [-46, 20, 8] and right IFG [46, 20, 8]). The left IFG source was not used in models M1-M6. Lines within a hemisphere represent forward and backward extrinsic connections. The inter-hemispheric line represents reciprocal lateral connections used in models M4-M6 and M10-M12. Not shown are bilateral intrinsic A1 connections present in all models. Lower left inset: The 12 models differed according to the number of sources (rows), the existence or absence of lateral connections and the types of connections that were allowed to vary in strength for the DCM calculations (F: forward, B: backward, L: lateral). For example, model M5 employed 5 sources and lateral STG connections but only forward and backward A1-STG and STG-IFG connections were allowed to change in connectivity strength in order to explain the difference in neuronal dynamics to standard and deviant tones. Middle inset: Model estimation based on all subjects (pooled data) suggesting that only 3 models (i.e., 7, 10 and 11) contribute to the data.

References

APA, 1994. Diagnostic and Statistical Manual of Mental Disorders, 4th. Edition. American Psychiatric Association

Arango, C., Fraguas, D., Parellada, M., 2014. Differential neurodevelopmental trajectories in patients with early-onset bipolar and schizophrenia disorders. Schizophr Bull 40 Suppl 2, S138-146.

Baldeweg, T., 2007. ERP repetition effects and mismatch negativity generation - A predictive coding perspecive. J Psychophysiol 21, 204-213.

Bennington, J.Y., Polich, J., 1999. Comparison of P300 from passive and active tasks for auditory and visual stimuli. Int J Psychophysiol 34, 171-177.

Braeutigam, S., Rose, S.P., Swithenby, S.J., Ambler, T., 2004. The distributed neuronal systems supporting choice-making in real-life situations: differences between men and women when choosing groceries detected using magnetoencephalography. Eur J Neurosci 20(1), 293-302.

Braeutigam, S., Swithenby, S.J., Bailey, A.J., 2008. Contextual integration the unusual way: a magnetoencephalographic study of responses to semantic violation in individuals with autism spectrum disorders. Eur J Neurosci 27(4), 1026-1036.

Coffman, B.A., Haigh, S.M., Murphy, T.K., Salisbury, D.F., 2017. Impairment in Mismatch Negativity but not Repetition Suppression in Schizophrenia. Brain Topogr 30, 521-530.

Cooray, G.K., Garrido, M.I., Brismar, T., Hyllienmark, L., 2016. The maturation of mismatch negativity networks in normal adolescence. Clin Neurophysiol 127(1), 520-529.

Dima, D., Frangou, S., Burge, L., Braeutigam, S., James, A.C., 2012. Abnormal intrinsic and extrinsic connectivity within the magnetic mismatch negativity brain network in schizophrenia: a preliminary study. Schizophr Res 135(1-3), 23-27.

Erickson, M.A., Ruffle, A., Gold, J.M., 2016. A Meta-Analysis of Mismatch Negativity in Schizophrenia: From Clinical Risk to Disease Specificity and Progression. Biol Psychiatry 79(12), 980-987.

Garrido, M.I., Kilner, J.M., Kiebel, S.J., Stephan, K.E., Friston, K.J., 2007. Dynamic causal modelling of evoked potentials: a reproducibility study. Neuroimage 36(3), 571-580.

Garrido, M.I., Friston, K.J., Kiebel, S.J., Stephan, K.E., Baldeweg, T., Kilner, J.M., 2008. The functional anatomy of the MMN: a DCM study of the roving paradigm. Neuroimage 42(2), 936-944.

Garrido, M.I., Kilner, J.M., Kiebel, S.J., Friston, K.J., 2009a. Dynamic causal modeling of the response to frequency deviants. J Neurophysiol 101(5), 2620-2631.

Garrido, M.I., Kilner, J.M., Kiebel, S.J., Stephan, K.E., Baldeweg, T., Friston, K.J., 2009b. Repetition suppression and plasticity in the human brain. Neuroimage 48(1), 269-279.

Garrido, M.I., Kilner, J.M., Stephan, K.E., Friston, K.J., 2009c. The mismatch negativity: a review of underlying mechanisms. Clin Neurophysiol 120(3), 453-463.

Gonzalez-Moreno, A., Aurtenetxe, S., Lopez-Garcia, M.E., del Pozo, F., Maestu, F., Nevado, A., 2014. Signal-to-noise ratio of the MEG signal after preprocessing. J Neurosci Meth 222, 56–61.

Haigh, S.M., Coffman, B.A., Salisbury, D.F., 2017. Mismatch Negativity in First-Episode Schizophrenia: A Meta-Analysis. Clin EEG Neurosci 48(1), 3-10.

Hermens, D.F., Chitty, K.M., Kaur, M., 2017. Mismatch negativity in bipolar disorder: A neurophysiological biomarker of intermediate effect? Schizophr Res (Article in Press).

Hill, S.K., Reilly, J.L., Keefe, R.S., Gold, J.M., Bishop, J.R., Gershon, E.S., Tamminga, C.A., Pearlson, G.D., Keshavan, M.S., Sweeney, J.A., 2013. Neuropsychological Impairments in Schizophrenia and Psychotic Bipolar Disorder: Findings from the Bipolar and Schizophrenia Network on Intermediate Phenotypes (B-SNIP) Study. Am J Psychiatry 170(11), 1275-1284.

Ivleva, E.I., Bidesi, A.S., Thomas, B.P., Meda, S.A., Francis, A., Moates, A.F., Witte, B., Keshavan, M.S., Tamminga, C.A., 2012. Brain gray matter phenotypes across the psychosis dimension. Psychiatry Res 204(1), 13-24.

Jahshan, C., Cadenhead, K.S., Rissling, A.J., Kirihara, K., Braff, D.L., Light, G.A., 2012a. Automatic sensory information processing abnormalities across the illness course of schizophrenia. Psychol Med 42(1), 85-97.

Jahshan, C., Wynn, J.K., Mathis, K.I., Altshuler, L.L., Glahn, D.C., Green, M.F., 2012b. Cross-diagnostic comparison of duration mismatch negativity and P3a in bipolar disorder and schizophrenia. Bipolar Disord 14(3), 239-248.

Johannesen, J.K., O'Donnell, B.F., Shekhar, A., McGrew, J.H., Hetrick, W.P., 2013. Diagnostic specificity of neurophysiological endophenotypes in schizophrenia and bipolar disorder. Schizophr Bull 39(6), 1219-1229.

Kaufman, J., Birmaher, B., Brent, D., Rao, U., Flynn, C., Moreci, P., Williamson, D., Ryan, N., 1997. Schedule for Affective Disorders and Schizophrenia for School-Age Children-Present and Lifetime Version (K-SADS-PL): initial reliability and validity data. J Am Acad Child Adolesc Psychiatry 36(7), 980-988.

Kaur, M., Battisti, R.A., Ward, P.B., Ahmed, A., Hickie, I.B., Hermens, D.F., 2011. MMN/P3a deficits in first episode psychosis: comparing schizophrenia-spectrum and affective-spectrum subgroups. Schizophr Res 130(1-3), 203-209.

Kaur, M., Lagopoulos, J., Lee, R.S., Ward, P.B., Naismith, S.L., Hickie, I.B., Hermens, D.F., 2013. Longitudinal associations between mismatch negativity and disability in early schizophrenia- and affective-spectrum disorders. Prog Neuropsychopharmacol Biol Psychiatry 46, 161-169.

Kay, S.R., Fiszbein, A., Opler, L.A., 1987. The positive and negative syndrome scale (PANSS) for schizophrenia. Schizophr Bull 13(2), 261-276.

Lee, K.W., Woon, P.S., Teo, Y.Y., Sim, K., 2012. Genome wide association studies (GWAS) and copy number variation (CNV) studies of the major psychoses: What have we learnt? Neurosci Biobehav Rev 36(1), 556-571.

Leucht, S., Samara, M., Heres, S., Patel, M.X., Furukawa, T., Cipriani, A., Geddes, J., Davis, J.M., 2015. Dose Equivalents for Second-Generation Antipsychotic Drugs: The Classical Mean Dose Method. Schizophr Bull 41(6), 1397-1402.

Li, J., Tang, Y., Womer, F., Fan, G., Zhou, Q., Sun, W., Xu, K., Wang, F., 2017. Two patterns of anterior insular cortex functional connectivity in bipolar disorder and schizophrenia. World J Biol Psychiatry, 1-9.

McCarley, R.W., Faux, S.F., Shenton, M.E., Nestor, P.G., Adams, J., 1991. Event-related potentials in schizophrenia: their biological and clinical correlates and a new model of schizophrenic pathophysiology. Schizophr Res 4(2), 209-231.

Näätänen, R., Gaillard, A.W., Mantysalo, S., 1978. Early selective-attention effect on evoked potential reinterpreted. Acta Psychol (Amst) 42(4), 313-329.

Näätänen, R., Kujala, T., Escera, C., Baldeweg, T., Kreegipuu, K., Carlson, S., Ponton, C., 2012. The mismatch negativity (MMN)--a unique window to disturbed central auditory processing in ageing and different clinical conditions. Clin Neurophysiol 123(3), 424-458.

Nagai, T., Kirihara, K., Tada, M., Koshiyama, D., Koike, S., Suga, M., Araki, T., Hashimoto, K., Kasai, K., 2017. Reduced Mismatch Negativity is Associated with Increased Plasma Level of Glutamate in First-episode Psychosis. Sci Rep 7(1), 2258.

O'Donnell, B.F., Vohs, J.L., Hetrick, W.P., Carroll, C.A., Shekhar, A., 2004. Auditory event-related potential abnormalities in bipolar disorder and schizophrenia. International journal of

psychophysiology : official journal of the International Organization of Psychophysiology 53(1), 45-55.

Oades, R.D., Wild-Wall, N., Juran, S.A., Sachsse, J., Oknina, L.B., Ropcke, B., 2006. Auditory change detection in schizophrenia: sources of activity, related neuropsychological function and symptoms in patients with a first episode in adolescence, and patients 14 years after an adolescent illness-onset. BMC Psychiatry 6:7.

Onitsuka, T., Oribe, N., Kanba, S., 2013. Neurophysiological findings in patients with bipolar disorder. Suppl Clin Neurophysiol 62, 197-206.

Oranje, B., Aggernaes, B., Rasmussen, H., Ebdrup, B.H., Glenthoj, B.Y., 2017. Selective attention and mismatch negativity in antipsychotic-naive, first-episode schizophrenia patients before and after 6 months of antipsychotic monotherapy. Psychol Med, 1-11.

Polich, J., 2007. Updating P300: An integrative theory of P3a and P3b. Cin Neurophysiol 118, 2128-2148.

Ribolsi, M., Mori, F., Magni, V., Codeca, C., Kusayanagi, H., Monteleone, F., Rubino, I.A., Siracusano, A., Bernardi, G., Centonze, D., Koch, G., 2011. Impaired inter-hemispheric facilitatory connectivity in schizophrenia. Clin Neurophysiol 122(3), 512-517.

Rudolph, E.D., Ells, E.M., Campbell, D.J., Abriel, S.C., Tibbo, P.G., Salisbury, D.F., Fisher, D.J., 2015. Finding the missing-stimulus mismatch negativity (MMN) in early psychosis: altered MMN to violations of an auditory gestalt. Schizophr Res 166(1-3), 158-163.

Salisbury, D.F., Shenton, M.E., McCarley, R.W., 1999. P300 topography differs in schizophrenia and manic psychosis. Biol Psychiatry 45(1), 98-106.

Salisbury, D.F., Kuroki, N., Kasai, K., Shenton, M.E., McCarley, R.W., 2007. Progressive and interrelated functional and structural evidence of post-onset brain reduction in schizophrenia. Arch Gen Psychiatry 64(5), 521-529.

Salisbury, D.F., Polizzotto, N.R., Nestor, P.G., Haigh, S.M., Koehler, J., McCarley, R.W., 2017. Pitch and Duration Mismatch Negativity and Premorbid Intellect in the First Hospitalized Schizophrenia Spectrum. Schizophr Bull 43(2), 407-416.

Tamminga, C.A., Ivleva, E.I., Keshavan, M.S., Pearlson, G.D., Clementz, B.A., Witte, B., Morris, D.W., Bishop, J., Thaker, G.K., Sweeney, J.A., 2013. Clinical phenotypes of psychosis in the Bipolar-Schizophrenia Network on Intermediate Phenotypes (B-SNIP). Am J Psychiatry 170(11), 1263-1274.

Taulu, S., Simola, J., Kajola, M., 2004. MEG recordings of DC fields using the signal space separation method (SSS). Neurol Clin Neurophysiol 35, 1-4.

Thibaut, F., Boutros, N.N., Jarema, M., Oranje, B., Hasan, A., Daskalakis, Z.J., Wichniak, A., Schmitt, A., Riederer, P., Falkai, P., Markers, W.T.F.o.B., 2015. Consensus paper of the WFSBP Task Force on Biological Markers: Criteria for biomarkers and endophenotypes of schizophrenia part I: Neurophysiology. World J Biol Psychiatry 16(5), 280-290.

Wang, Y., Jia, Y., Feng, Y., Zhong, S., Xie, Y., Wang, W., Guan, Y., Zhu, D., Huang, L., 2014. Overlapping auditory M100 and M200 abnormalities in schizophrenia and bipolar disorder: a MEG study. Schizophr Res 160(1-3), 201-207.

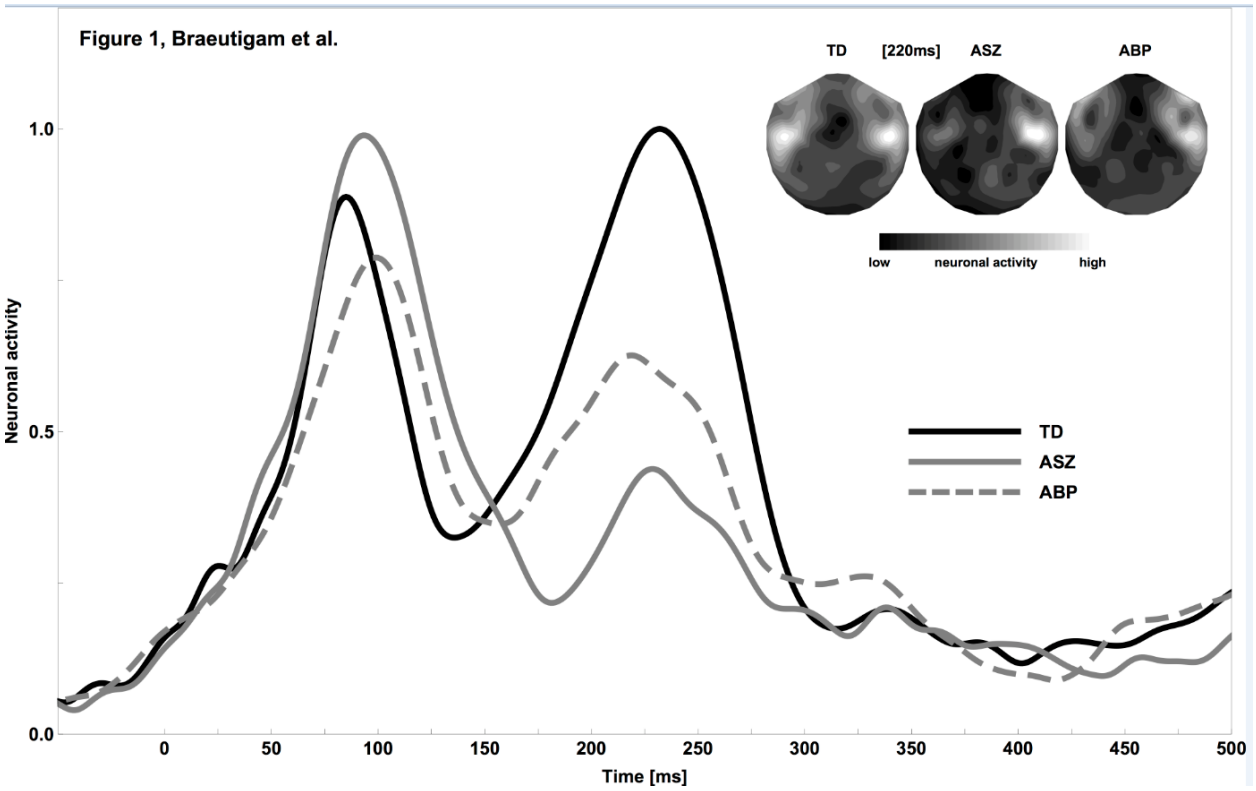
Figure 1, Braeutigam et al.
TD
[220ms]
ASZ
ABP
low
neuronal activity
high
TD
ASZ
ABP
Neuronal activity
1.0
0.5
0.0
0
50
100
150
200
250
300
350
400
450
500
Time [ms]

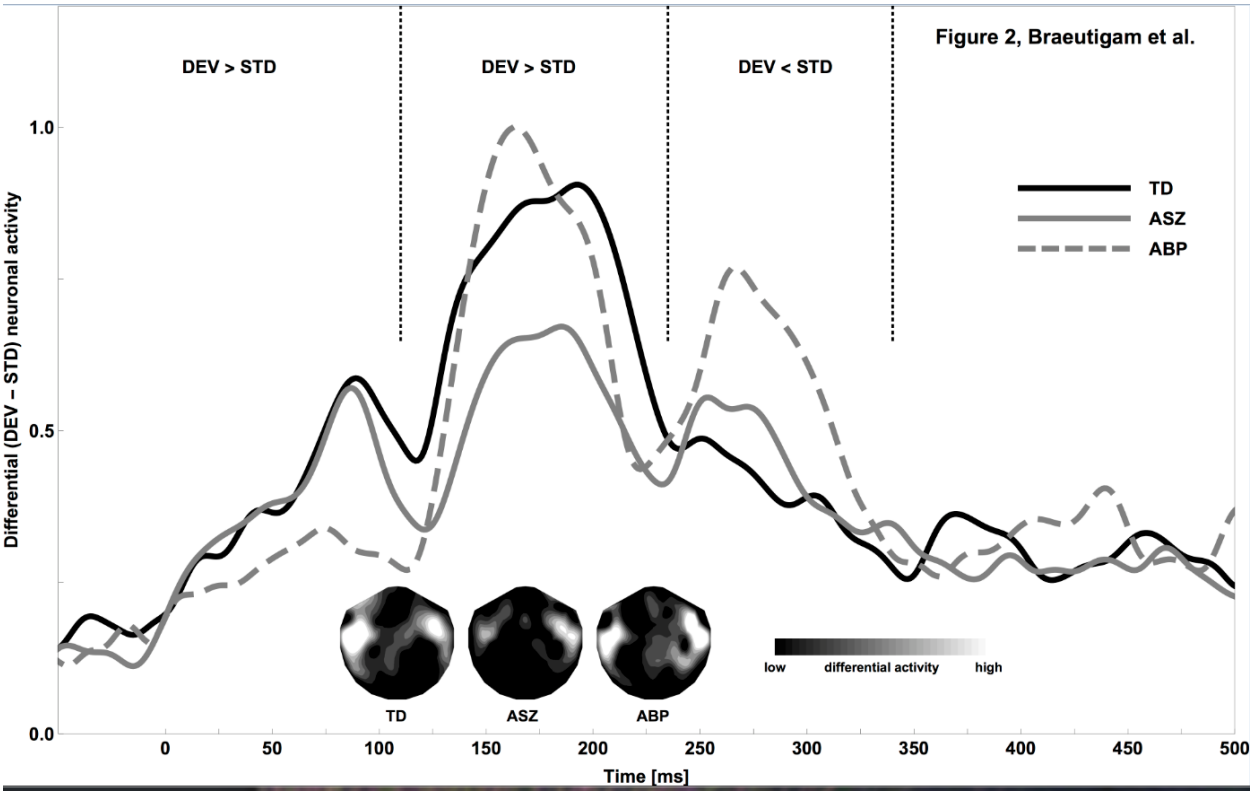
Figure 2, Braeutigam et al.
DEV > STD
DEV > STD
DEV < STD
TD
ASZ
ABP
Differential (DEV – STD) neuronal activity
1.0
0.5
0.0
low
differential activity
high
TD
ASZ
ABP
0
50
100
150
200
250
300
350
400
450
500
Time [ms]

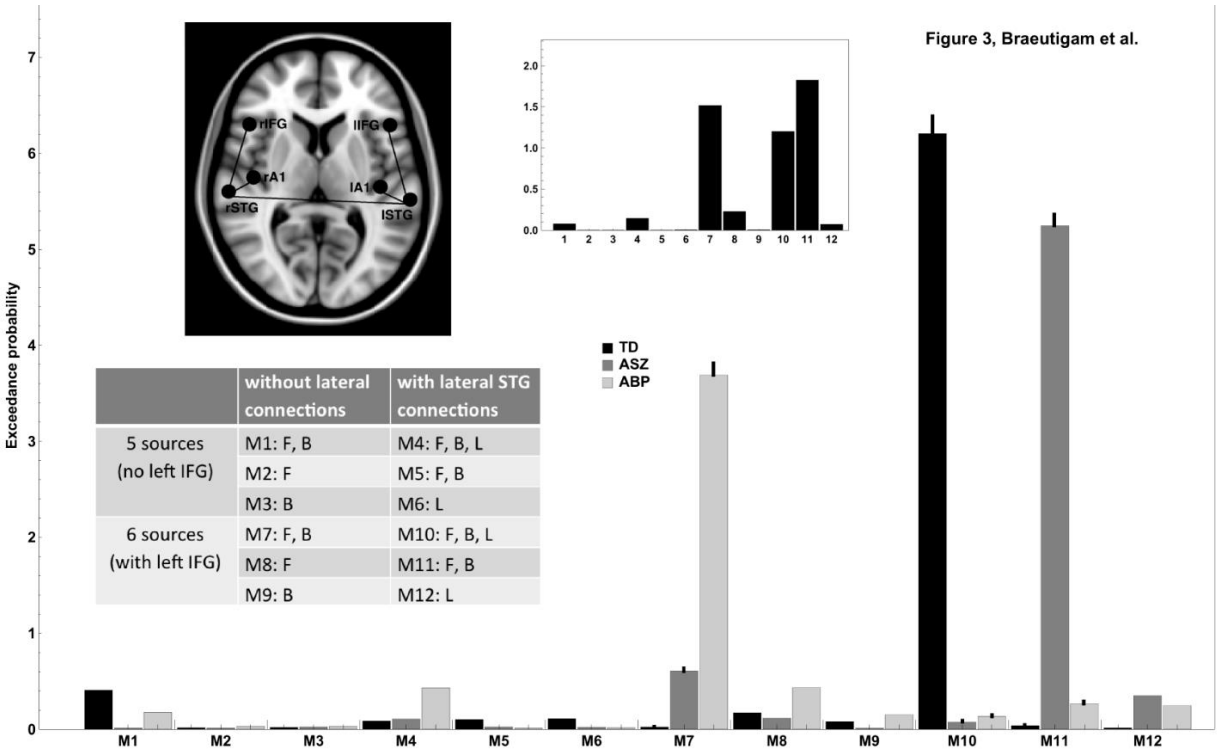

	without lateral connections	with lateral STG connections
5 sources (no left IFG)	M1: F, B	M4: F, B, L
	M2: F	M5: F, B
	M3: B	M6: L
6 sources (with left IFG)	M7: F, B	M10: F, B, L
	M8: F	M11: F, B
	M9: B	M12: L

Supplementary material

S1 Illustration of the roving tone sequence used in this experiment. Tones of 70ms duration are denoted by vertical bars, where bar height reflects tone frequency. In a roving paradigm, each tone has the same overall rate of occurrence. Tone trains of length 1 to 11 were used but only trains of equi-probable (0.125) lengths 6 – 11 entered the analysis. Deviant (DEV): first tone in train. Standard (STD): sixth tone in train.

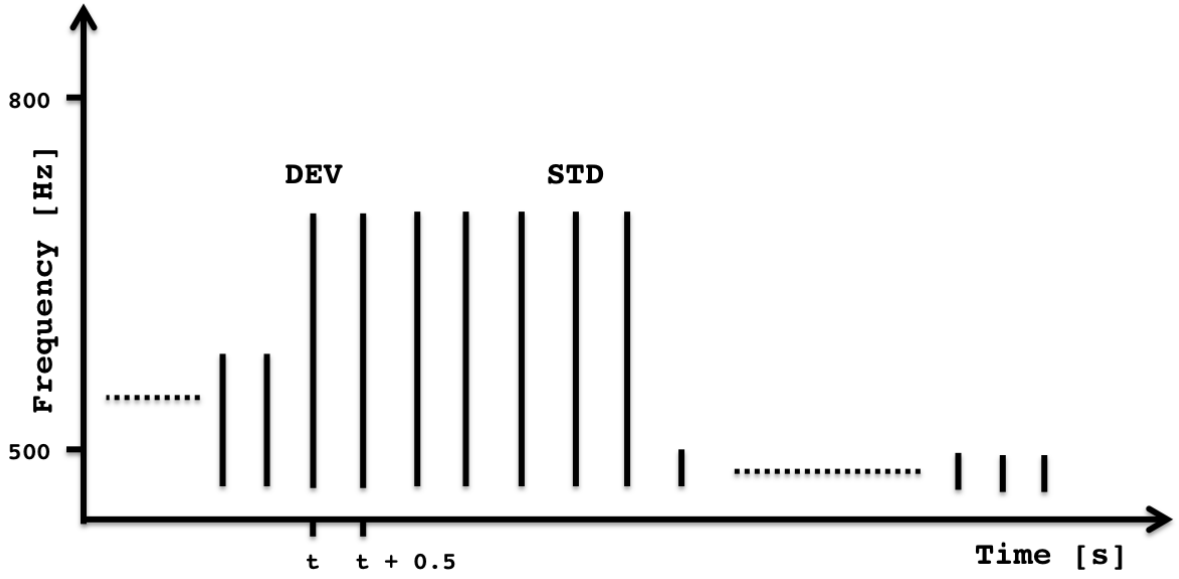

S2 Core DCM parameter used for analysis (Matlab™ format).

5 sources

Same as for 6 sources (below) but no left IFG source and no connection that either originate or terminate in left IFG. Corresponding models are M1 -> M7, M2 -> M8, .., M6 -> M12.

6 sources

```
DCM                  = [];
DCM.xY.modality      = 'MEGPLANAR';
DCM.options.analysis = 'ERP';
DCM.options.model    = 'ERP';
DCM.options.spatial  = 'ECD';
DCM.options.trials   = [1 2];
DCM.options.Tdcm(1)  = 0;
DCM.options.Tdcm(2)  = 250;
DCM.options.Nmodes   = 8;
DCM.options.h        = 1;
DCM.options.onset    = 60;
DCM.options.D        = 1;
DCM.M                = struct('nograph', 1);

DCM                  = spm_dcm_erp_data(DCM);
DCM.Lpos             = [ [-42; -22; 7], ...
                         [ 46; -14; 8], ...
                         [-61; -32; 8], ...
                         [ 59; -25; 8], ...
                         [-46;  20; 8], ...
                         [ 46;  20; 8]];
DCM.Sname            = { 'left A1',   ...
                         'right A1',  ...
                         'left STG',  ...
                         'right STG', ...
                         'left IFG',  ...
```

```
                        'right IFG'};
Nareas                = size(DCM.Lpos,2);


DCM                   = spm_dcm_erp_dipfit_p(DCM);
DCM.xU.X              = [0; 1];
DCM.xU.name           = {'deviant'};


DCM.A = [];
DCM.B = [];
DCM.C = [];


% forward
DCM.A{1}      = zeros(Nareas, Nareas);
DCM.A{1}(3,1) = 1;
DCM.A{1}(4,2) = 1;
DCM.A{1}(5,3) = 1;
DCM.A{1}(6,4) = 1;
% backward
DCM.A{2}      = zeros(Nareas,Nareas);
DCM.A{2}(1,3) = 1;
DCM.A{2}(2,4) = 1;
DCM.A{2}(3,5) = 1;
DCM.A{2}(4,6) = 1;
% lateral
DCM.A{3}      = zeros(Nareas,Nareas);
% input
```

```
DCM.C         = [1; 1; 0; 0; 0; 0];


switch model % requested by the calling function
    case 'M7:FB'
        DCM.B{1}      = DCM.A{1} + DCM.A{2};
        DCM.B{1}(1,1) = 1;
        DCM.B{1}(2,2) = 1;


    case 'M8:F'
        DCM.B{1}      = DCM.A{1};
        DCM.B{1}(1,1) = 1;
        DCM.B{1}(2,2) = 1;


    case 'M9:B'
        DCM.B{1}      = DCM.A{2};
        DCM.B{1}(1,1) = 1;
        DCM.B{1}(2,2) = 1;


    case 'M10:FBLm'
        DCM.A{3}(4,3) = 1;
        DCM.A{3}(3,4) = 1;


        DCM.B{1}      = DCM.A{1} + DCM.A{2} + DCM.A{3};
        DCM.B{1}(1,1) = 1;
        DCM.B{1}(2,2) = 1;
```

```
    case 'M11:FBL'
        DCM.A{3}(4,3) = 1;
        DCM.A{3}(3,4) = 1;

        DCM.B{1}      = DCM.A{1} + DCM.A{2};
        DCM.B{1}(1,1) = 1;
        DCM.B{1}(2,2) = 1;

    case 'M12:L'
        DCM.A{3}(4,3) = 1;
        DCM.A{3}(3,4) = 1;

        DCM.B{1}      = DCM.A{3};
        DCM.B{1}(1,1) = 1;
        DCM.B{1}(2,2) = 1;
end
```

S3 Bootstrap test for exceedance probabilities. For each subject and model, DCM connection estimates were calculated using the parameters given in S2. Subsequently, the Bayesian Model Estimator (SPM8) routine was repeated 500 times for each subject group separately. On each iteration N (14, 15, or 16) subjects were randomly drawn (with replacement) from the group pool. Finally, the bootstrap replications served to estimate the mean exceedance probability and is standard error for each group.